

An experimental study on the effect of CFRP on behavior of reinforce concrete beam column connections

Qiang Xie^{1,2}, Hamid Sinaei³, Mahdi Shariati⁴,
Majid Khorami⁵, Edy Tonnizam Mohamad⁶ and Dieu Tien Bui^{*7}

¹ School of Civil Engineering, Central South University, Changsha, Hunan 410075, China

² Hunan City University, Yiyang, Hunan 413000, China

³ Department of Civil Engineering, Sirjan Branch, Islamic Azad University, Sirjan, Iran

⁴ Faculty of Civil Engineering, University of Tabriz, Tabriz, Iran

⁵ Universidad UTE, Facultad de Arquitectura y Urbanismo, Calle Rumipamba s/n y Bourgeois, Quito, Ecuador

⁶ Centre of Tropical Geoengineering (GEOTROPIK), Faculty of Civil Engineering, Universiti Teknologi Malaysia, Johor Bahru, Malaysia

⁷ Institute of Research and Development, Duy Tan University, Da Nang 550000, Vietnam

(Received September 8, 2018, Revised February 16, 2019, Accepted March 3, 2019)

Abstract. The aim of this research is reinforcing of concrete with variety of fiber reinforced polymer (FRP) configurations and investigates the load capacity and ductility of these connections using an experimental investigation. Six scaled-down RC exterior joints were tested under moderately monotonic loads. The results show that, the shape of the FRP had a different effect on the joint capacity and the connection ductility coefficient. The greatest effect on increasing the ductility factor was seen in the sample where two reinforcement plates were used on both sides of the beam web (RCS5 sample). For the sample with the presence of FRP plates at the top and bottom of the beam (RCS3 sample), the ductility factor was reduced even the load capacity of this sample increased. Except for the RCS3 sample, the rest of the samples exhibited an increase in the ductility factor due to the FRP reinforcement.

Keywords: CFRP plate; plastic hinge relocation; finite element; rehabilitation; strengthening

1. Introduction

Rehabilitating and strengthening old or pre-damaged building structures and bridges comprising Reinforced Concrete (RC) present vexatious challenges for structural design engineers. It is not always to replace deficient structures due to high expenses and usage limitations (Ardalan *et al.* 2009, Wang *et al.* 2018, 2019, Zhou *et al.* 2019). Thus, structures built several decades ago may need strengthening and upgrading to meet current service load demands. Strengthening and retrofitting programs are more reasonable compared to demolishing and rebuilding structures in terms of service disruption, labor and material costs (Tang *et al.* 2006, Hadi and Tran 2016, Shahabi *et al.* 2016a, Shariati *et al.* 2016, Bezerra *et al.* 2018). The required strength and serviceability performance of a strengthened structure is only achievable by completely understanding the materials' behavior and strengthening techniques used (Daly and Witarnawan 1997, Nordin 2005, McCormac and Brown 2015). Several methods of strengthening RC structures containing various materials have been studied and applied in the rehabilitation field. The most recent type of material utilized for strengthening purposes in modern times is Fiber-Reinforced Polymer

(FRP) composite (Aslam *et al.* 2015). Advantages of FRP that supersede traditional strengthening materials are said to be sufficient resistance to rust, excellent strength as compared to the self-weight, user-friendliness and neutrality to electromagnetic forces. All these benefits strongly encourage FRP use for RC structure strengthening, especially in cases where traditional steel reinforcement fails to provide the required serviceability (Aslam *et al.* 2015). Strengthening with FRP composites is one of the more recent retrofitting and strengthening techniques (Engindeniz *et al.* 2005).

Rehabilitating and strengthening old or pre-damaged building structures and bridges comprising Reinforced Concrete (RC) present vexatious challenges for structural design engineers. It is not always to replace deficient structures due to high expenses and usage limitations. Thus, structures built several decades ago may need strengthening and upgrading to meet current service load demands. Strengthening and retrofitting programs are more reasonable compared to demolishing and rebuilding structures in terms of service disruption, labor and material costs (Tang *et al.* 2006, Hadi and Tran 2016). The required strength and serviceability performance of a strengthened structure is only achievable by completely understanding the materials' behavior and strengthening techniques used (Daly and Witarnawan 1997, Nordin 2005, Bazzaz *et al.* 2015, Fanaie *et al.* 2015, McCormac and Brown 2015, Safa *et al.* 2016).

Several methods of strengthening RC structures

*Corresponding author, Ph.D.,
E-mail: BuiTienDieu@gmail.com

containing various materials have been studied and applied in the rehabilitation field specifically for composite beams with different types of shear connectors by the authors (Shariati *et al.* 2011, 2012a, b, c, 2014, 2015, 2016, 2017, Shariati 2013, Mohammadhassani *et al.* 2014, Khorramian *et al.* 2015, 2017, Arabnejad *et al.* 2016, Shahabi *et al.* 2016a, b, Tahmasbi *et al.* 2016, Hosseinpour *et al.* 2018, Ismail *et al.* 2018, Nasrollahi *et al.* 2018, Sadeghipour-*et al.* 2018, Sedghi *et al.* 2018, Wei *et al.* 2018). The most recent type of material utilized for strengthening purposes in modern times is Fiber-Reinforced Polymer (FRP) composite (Aslam *et al.* 2015). Advantages of FRP that supersede traditional strengthening materials are said to be sufficient resistance to rust, excellent strength as compared to the self-weight, user-friendliness and neutrality to electromagnetic forces. All these benefits strongly encourage FRP use for RC structure strengthening, especially in cases where traditional steel reinforcement fails to provide the required serviceability (Aslam *et al.* 2015). Strengthening with FRP composites is one of the more recent retrofitting and strengthening techniques (Engindeniz *et al.* 2005). Another major contributor to beam-column joint failure is the so-called “strong beam/weak column” philosophy from the 1960s and 1970s. The use of FRPs for strengthening RC structures has become increasingly popular over the last two decades due to material cost reductions, versatility and benefits as well as the ability to significantly improve member strength, fatigue life and serviceability. Among FRPs, Carbon Fiber-Reinforced Polymer (CFRP) composites are used most frequently in the construction industry because they generally contain high-performance carbon fibers placed in the resin matrix. Statistics reveal that among various FRP types, CFRP contributes to 95% of usage for deficient RC structure strengthening (Aslam *et al.* 2015). One of the primary reasons is that this composite can easily bond externally to RC elements.

A poor frame design enhances the chances of plastic hinge formation in the column, which would make the column fail at lower ultimate loads as well as reduce the column’s energy dissipation capability that is dependent on axially applied load and reinforcement design (Thomas and Priestley 1992). A way to mitigate this problem is to design DMR frames based on the strong-column-weak-beam design. This method of designing members allows both the connection and the column to remain in elastic stage when

the lateral load intensity is higher than in normal situations. Moreover, most energy dissipation occurs within the plastic hinge formed in the beam.

The current study focuses on experimental analyses of RC BCC strengthening using different CFRP composite configurations. The behavior of RC BCCs reinforced externally with innovative CFRP composite elements under static loading is primarily investigated. This involves wrapping and attaching CFRP plies around the connection area. This study will determine how various CFRP configurations affect the performance of strengthened RC BCCs as connections. The validity of these innovative external reinforcement systems is verified by comparing the experimental results with nonlinear finite element modelling results.

Since column confinement with concrete or steel jacketing is labor-intensive and adds considerable weight to the elements, it is always desirable to use cost-effective, durable and fast techniques such as externally bonded CFRP composite laminates for the rehabilitation of existing structures. One of the main goals of this research is to determine the appropriate length and thickness of carbon fiber-reinforced plastic (CFRP) reinforcement panel plates in order to improve beam-column concrete connections to have the greatest impact on the plastic hinge transfer from within the connection toward the concrete beam.

2. Experimental test

2.1 Specimen design and geometry

The test specimens were six 1:2.2 scale models of the prototype. All joints consisted of 180 mm wide and 230 mm deep beams with 220 mm × 180 mm columns. The reinforcement consisted of R6 (D = 6 mm) ties with f_y of 400 MPa and N12 (D = 12 mm) main bars with f_y of 500 MPa and yield strain of 0.003 mm/mm. The carbon fiber reinforced plastic (CFRP) sheets utilized in all experiments were unidirectional with ultimate stress of 3500 MPa, ultimate strain of 0.017 mm/mm and constant modulus of 210 GPa. The concrete had compressive strengths of 40.1, 40.3, 41.5, 41.3, 39.2 and 39.3 MPa in the plain (RCS1) and retrofitted specimens (RCS2, RCS3, RCS4, RCS5 and RCS6), respectively.

Both sides of the column as well as the back of the beam

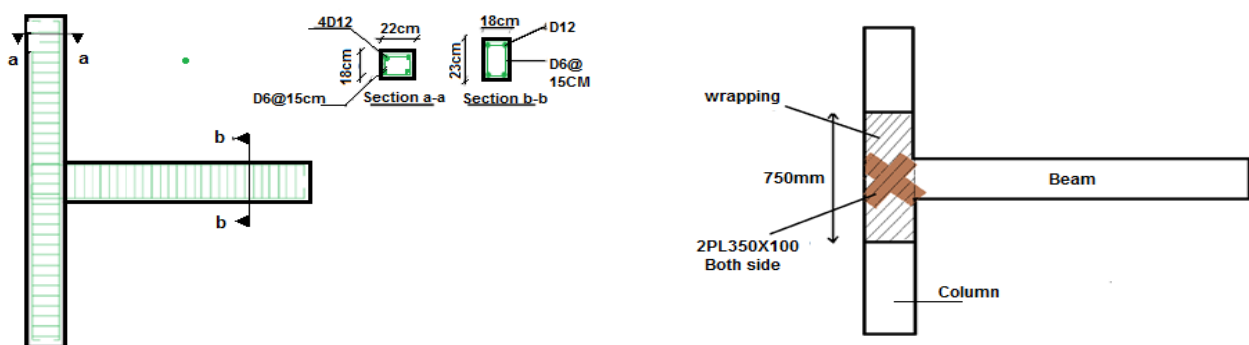


Fig. 1 Details and geometry of control specimen and CFRP configuration of specimen RCS2

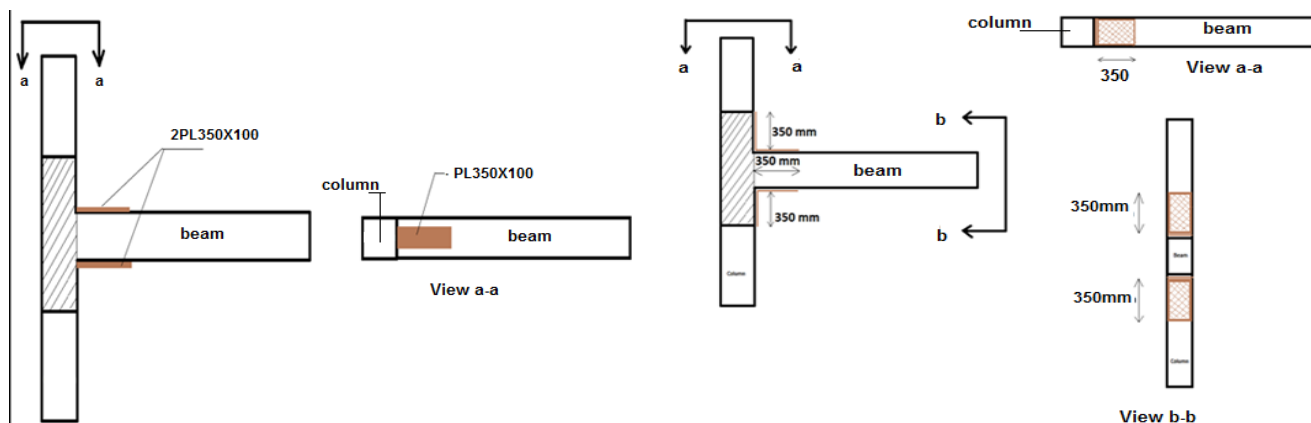


Fig. 2 CFRP configuration of specimen RCS3 and CFRP configuration of specimen RCS4

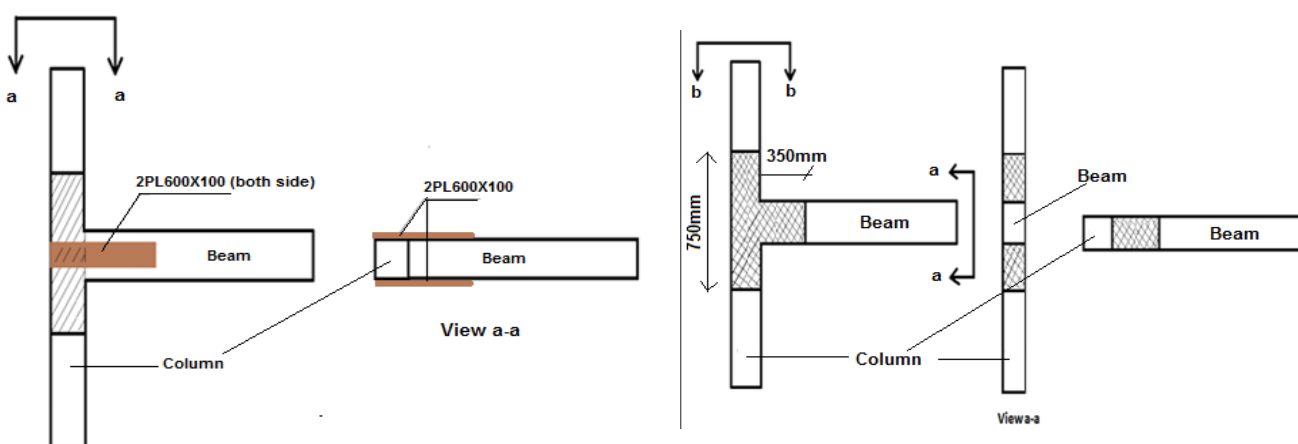


Fig. 3 CFRP configuration of specimen RCS5 and CFRP configuration of specimen RCS6

were wrapped with CFRP. The CFRP plate ends were also wrapped in order to provide CFRP anchorage. It should be mentioned that in a real structure, this can be achieved using a bolted CFRP system as reported by Oehlers is covered by Australian standard guidelines at present. All the specimens were subjected to axial loading and the corresponding ratio was about 20% of the column capacity (0.20Agfc), which is a practical range in real frame

buildings (Hui and Irawan 2001, Hwang and Lee 1999). The specimens' geometries and CFRP configurations are shown in Figs. 1 to 3.

2.2 Specimen construction

The specimens were fabricated at the University of Malaya Structural Engineering Laboratory. For ease of



Fig. 4 Concrete specimen casting and strain gauge installation

construction, the specimens were made and cased in a flat position, as shown in Fig. 4.

After assembling the reinforcement rebar and installing the strain gauges, the concrete was cast with 80 mm slump and compacted as indicated in Figs. 5 to 8. Concrete cylinders were taken from the cast concrete batch to test the concrete's compressive strength. The specimens were left to cure for 28 days in a controlled environment. Prior to the tests, the specimens were lifted using a crane and transferred to The Construction Industry Development (CIDB) laboratory by truck.

2.3 Material properties

2.3.1 Concrete

The six specimens evaluated in this study were cast in three groups due to laboratory space limitations. The average compressive strengths of concrete in the first, second and third groups after 28 days and on the day of the test are presented in Table 1. The variation in compressive strength among these groups was considered acceptable since the difference was less than 5% on test day.



Fig. 5 Concrete specimen casting and concrete slump measurement



Fig. 6 Concrete cylinders for testing the material properties and Installation of CFRP plate on specimen RCS2

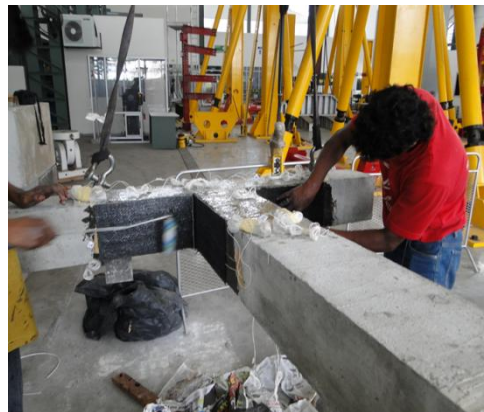


Fig. 7 Installation of CFRP plate on specimen RCS3 and Installation of CFRP sheet on specimen RCS4



Fig. 8 Installation of CFRP plate on specimen RCS5 and CFRP wrapping of specimen RCS6

Table 1 Concrete properties

Average compressive strength (Day of Test) (MPa)	Average compressive strength (28 Days) (MPa)	Specimens
40.2	38.9	First Group (RCS1&RCS2)
41.4	40.2	Second Group (RCS3&RCS4)
39.3	38.1	Third Group (RCS5&RCS6)

Table 2 Mechanical properties of reinforcement steel

Ultimate stress (MPa)	Yield stress (MPa)	
600	400	#6 Rebar
700	500	#12 Rebar



Fig. 9 Position of 500 kN actuator

2.3.2 Steel reinforcement

All reinforcement rebars used in this research study were grade A615. The reinforcement tensile properties were tested according to ASTM A370. The mechanical properties of the reinforcement steel are presented in Table 2.

2.3.3 FRP composite laminate

The composite laminates evaluated in this study were tested according to ASTM D-3039-08 to determine their mechanical properties. The carbon fiber reinforced plastic (CFRP) sheets used in all experiments were unidirectional with ultimate stress of 3500 MPa, ultimate strain of 0.017 mm/mm and constant modulus of 210 GPa.

2.4 Test setup

Schematic views of the main test setup are shown in Figs. 9 and 10. The specimens were placed in the setup such that the column longitudinal axis was vertical and the beam longitudinal axis was horizontal. A rigid steel column cap was used for the top end. Each column end was fit inside the cap using a steel plate of appropriate thickness to prevent movement between the cap and the column end. To

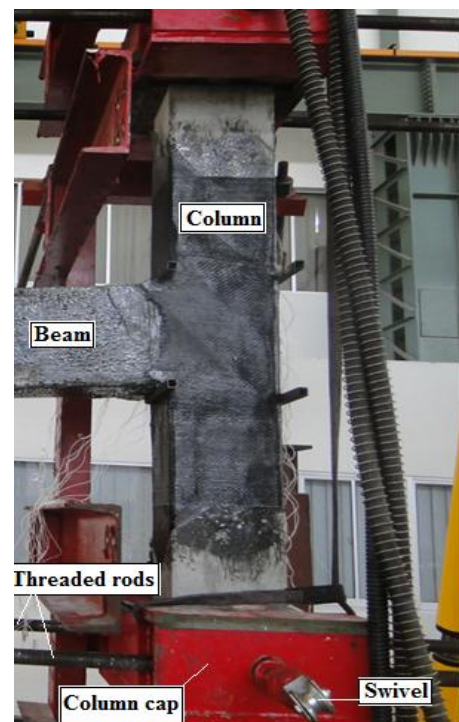


Fig. 10 Specimen installation

produce the pinned connection for the column ends, a steel roller was welded to the caps. The column caps were supported in the loading plane using high-strength threaded rods, which were attached to the strong support from one side and connected to the caps by special swivels on the other side. The swivels allowed the specimens to rotate fully on the plane of loading. The threaded rods were pre-loaded during specimen installation to prevent lateral movement of the specimens. The column caps were also supported by a strong frame, which was restrained to the solid floor by lateral threaded rods. Special bearings connected the caps to the frame. This frame prevented out-of-plan lateral displacement of the column and also restrained the 2000 kN actuator. The beam was restrained in the lateral direction to prevent lateral tensional buckling. All specimens underwent two loading steps. In step one; the column was loaded with a constant axial load applied by a 2,000 kN hydraulic actuator to determine the upper floors' reaction. The axial load value was kept constant during the rest of the test. In step two, one vertical load was applied at the beam end to simulate the deformed shape of a similar connection in a building subjected to lateral loads. The beam load was applied using a 500 kN actuator. Displacement control was used to apply monotonic deflection in small increments until the specimens failed.

3. Experimental results

3.1 General

After the six beam-column joint specimens were designed and constructed, they were tested. During each test, the cracking progress was recorded at each loading level and pictures were taken at the end of loading. The experimental tests on specimens RCS1 to RCS6 are explained in this chapter. In the first loading step, a constant axial load of 300 kN was applied to the column and maintained until the end of the test. In the second step, the beam end was loaded downward. The specimens' behavior is presented in terms of load-displacement relationship, failure modes and strain at different locations on the specimens. This data provides valuable information on the behavior and progress of failure in the specimens. Selected data is also useful for understanding the behavior of members and possible failure modes. The results are described for each specimen individually. The results are discussed by comparing the experimental test results for the specimens to identify their performance.

3.2 Specimen behavior

In the control specimen (RCS1), flexural cracking of the beam section subjected to maximum bending moment initially appeared at a beam tip load of 6.7 kN. Cracks were detected simultaneously beside the beam close to the column. The onset of diagonal cracks in the joint area took place at a beam tip load of 10 kN. Additional cracks in the joint area appeared thereafter as loading progressed but remained within a very fine width throughout the test. The

beam's longitudinal steel yielded at an average beam tip load of 12 kN and the corresponding average yield displacement (D_y) was 34 mm. Subsequently, the beam cracked extensively along a distance shorter than its depth from the column face. Finally, wide cracks developed in the hinge area at a beam tip load of 12.8 kN and the test was stopped as the beam capacity dropped substantially.

In specimen RCS2, two cross-shaped CFRP plates were bonded on both sides of the beam-column joint in the vertical plane, and then the column was wrapped around the joint. RCS2 was loaded until the first flexural crack was detected at a beam section adjacent to the column, which took place at a load of about 7.5 kN. Cracks were detected simultaneously on the beam end. As the loading proceeded, cracking progressed in the beam segment adjacent to the column and intensified due to the combination of high shear and normal stresses in this section. The degradation in strength progressed and the test was stopped at a load of about 19.1 kN.

Throughout the test, read strain on the FRP members indicated that their behavior remained elastic and did not fail.

Specimen RCS3 was retrofitted with two CFRP plate added to top and bottom of beam and the column were wrapped with CFRP on both sides as well as around the back of the beam. The CFRP plate ends were also wrapped in order to provide CFRP anchorage. The onset of diagonal cracks at the beam sides took place at a load of 6.5 kN. Additional cracks with uniform spacing appeared thereafter as loading progressed but remained within a very fine width throughout the test. At a load of 17 kN, the beam cracked extensively along a distance equal to its depth from the column face. The beam's transverse steel yielded at an average beam tip load of 16 kN and the cracks grew deeper. Then wide cracks developed in the area where the CFRP plate was connected to the beam, rubble began falling, and the beam lost most of its concrete. Hence, CFRP plate debonding occurred, stress in the longitudinal rebar suddenly increased and the rebar yielded at a load of 16.1 kN. The test was stopped as the beam capacity dropped substantially at a maximum recorded load of 17.81 kN.

Sample RCS4 was reinforced at the top and bottom corners of the connection with the L-shaped CFRP sheet layers, as described in Chapter 3. The CFRP layers on the beam caused the first bending cracks on the beam to shift to the closest region without CFRP to the column. At greater loading, diagonal cracks formed within the beam due to shear stress. Most cracks were at a distance with the beam depth from the column. As the loading further increased, the cracks grew wider and caused the transverse rebar to yield. Subsequently, the longitudinal rebar yielded at a suitable distance from the column. With transverse rebar yielding the cracks intensified, the CFRP layers ruptured and finally, an ultimate load (F_u) of 18.15 kN was recorded.

Despite a significant increase in loading capacity, the ductility did not increase effectively due to shearing strength weakness. Evidently, it is possible to increase the ductility by selecting a suitable thickness for the CFRP layer. Moreover, selecting a suitable CFRP length can have an important role in determining the location and time of

plastic hinge formation. This topic will be addressed in further sections via numerical analysis.

For sample RCS5, two reinforcing CFRP plates were used on both sides of the beam web. The first bending crack started at $F = 5.5$ kN and the shear stress increased, but on account of the CFRP plates, shear cracking was controlled. At higher loads, new cracks formed paralleled to the beam.

According to strain gauge data, the top beam rebars yielded. The location where a plastic hinge formed was not sufficiently far from the column; therefore, by choosing suitable CFRP plate lengths and optimizing the CFRP thickness, it is possible to predict a more appropriate point on the beam for plastic hinge formation. The CFRP plates helped control the shear stress while the shear resistance of specimen RCS5 rose. The maximum stress of the longitudinal rebar reduced and the specimen became more ductile.

In the last sample, RCS6, in the vicinity of the joint, both beam and column were wrapped. A CFRP wrap covered the beam by around 35 cm near the joint. Due to the vertical presence of CFRP in this sample the shear strength increased, while CFRP located on top of the beam helped increment the bending strength. With increasing load the bending stress increased. Moreover, the present CFRP layers controlled the bending stresses of the steel close to the column, and the longitudinal rebars yielded at an acceptable distance from the column.

It was observed that sample RCS6 exhibited significant ultimate load due to the adequate shear and bending strength function. The strain gauges indicated that the plastic hinge formed sufficiently far from the column; therefore, by opting for a suitable beam length in reinforcing with CFRP and optimizing the CFRP thickness, it became possible to create a suitable point on the beam for plastic hinge formation.

3.3 Ductility factor and ultimate load

The first yield of the reinforcement rebar was calculated and determined based on data recorded for the beam and column section. When the data logger recorded the first yield that occurred to any of the steel reinforcement rebars,

Table 3 Summary of experimental test results

Specimen	FY	FU	DY	DU	μ	Increase in strength
RCS1	12	12.8	34	65	1.91	0
RCS2	16.6	19.1	35	90	2.57	49%
RCS3	16.1	17.81	47.5	82	1.73	39%
RCS4	14.7	18.15	28.4	62.18	2.19	42%
RCS5	18.2	21.86	21.8	85	3.9	71%
RCS6	21.29	23.15	22.9	76.61	3.69	81%

the corresponding displacement (D_y) was measured. The data logger also recorded displacement corresponding to ultimate load (D_u). D_y and D_u were used to calculate the experimental ductility factor (μ). The ductility factor is calculated with Eq. (1)

$$\mu = \frac{D_u}{D_y} \quad (1)$$

The ductility factor values for all specimens are given in Table 3.

The control specimen (RCS1) was tested by loading and the data logger measured its ultimate load. Then specimens RCS2-RCS6 were reinforced with various CFRP forms and tested. Reinforcing the specimens increased their ultimate loads significantly. A summary of the ultimate loads and strength increment is presented in Table 3.

3.4 Load-displacement curve

In the test, a data logger recorded the load and corresponding displacement. Fig. 11 displays the load variations against displacement for all specimens. The presence of CFRP reinforcement affected the ultimate load and ductility factor of the specimens.

3.5 Remark and discussion

As the results in the previous sections revealed, applying

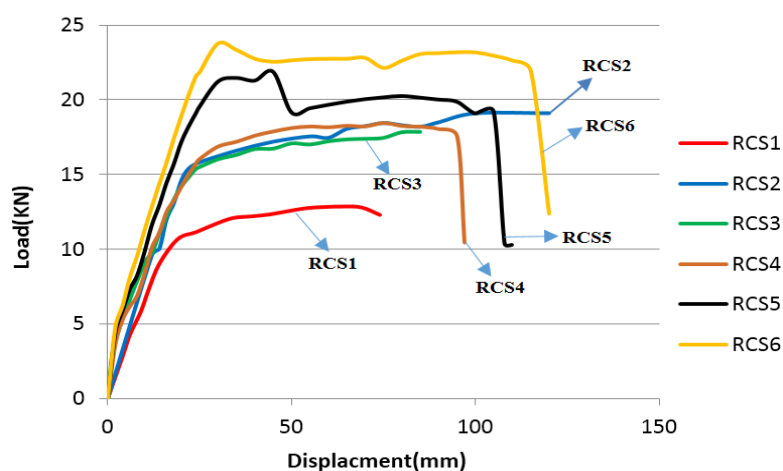


Fig. 11 The load-displacement diagram of RCS6 sample

CFRP reinforcement increased the beam-column connection's load capacity in all specimens. Nonetheless, the load capacity increase rate varied for each sample according to the geometry and location of the CFRP reinforcement applied. The CFRP dimensions had a different effect on the connection ductility factor. Accordingly, the presence of CFRP plates on the top and bottom of the beam in the RCS3 sample reduced the ductility factor, but the load capacity of this sample increased. The greatest effect on the increase in ductility factor was seen for sample RCS5, where two reinforcement plates were used on both sides of the beam web. Except for sample RCS3, the others exhibited an increment in the ductility factor due to the reinforcement. The reinforcement plates in the beam web influenced the ductility factor increment considerably. On the other hand, sample RCS6, in which parts of the beam and column at the top and bottom of the connection point were wrapped with CFRP layers, performed well. Unfortunately, implementing CFRP reinforcement in the forms of samples RCS2 and RCS6 is not applicable in practice due to the three-dimensional structure of actual concrete frames and the presence of frames perpendicular to the frame concerned. Hence, to examine the most effective form of reinforcement, only the RCS3 and RCS5 sample models are studied in upcoming sections, whereby the CFRP reinforcement varies in length and thickness.

4. Conclusions

In the experimental program, six scaled-down RC exterior joints were tested under moderately monotonic loads. One specimen was the control while the five other specimens were strengthened with CFRP of various designs. Applying the CFRP reinforcement increased the load capacity of the beam-column connections in all specimens. The ductility factor of sample RCS3 (CFRP plates on the top and bottom of the beam) reduced smoothly, but the ductility factor of the other samples increased. The greatest effect on the ductility factor was seen in sample RCS5 (almost 100%), where two reinforcement plates were bonded to both sides of the beam web.

References

- Ardalan, H., Eslami, A. and Nariman-Zadeh, N. (2009), "Piles shaft capacity from CPT and CPTu data by polynomial neural networks and genetic algorithms", *Comput. Geotech.*, **36**(4), 616-625.
- Arabnejad, K.M.M., Ramli Sulong, N.R., Shariati, M. and Tahir, M.M. (2016), "Investigation of through beam connection to concrete filled circular steel tube (CFCST) column", *J. Constr. Steel Res.*, **121**, 144-162.
- Aslam, M., Shafiq, P., Jumaat, M.Z. and Shah, S.N.R. (2015), "Strengthening of RC beams using prestressed fiber reinforced polymers—A review", *Constr. Build. Mater.*, **82**, 235-256.
- Bazzaz, M., Andalib, Z., Kheyroddin, A. and Kafi, M.A. (2015), "Numerical comparison of the seismic performance of steel rings in off-centre bracing system and diagonal bracing system", *Steel Compos. Struct., Int. J.*, **19**(4), 917-937.
- Bezerra, L.M., Barbosa, W.C., Bonilla, J. and Cavalcante, O.R. (2018), "Truss-type shear connector for composite steel-concrete beams", *Constr. Build. Mater.*, **167**, 757-767.
- Daly, A. and Witarnawan, W. (1997), "Strengthening of bridges using external post-tensioning", Paper PA3307/97, Transportation Research Laboratory, Berkshire, UK.
- Engindeniz, M., Kahn, L.F. and Abdul-Hamid, Z. (2005), "Repair and strengthening of reinforced concrete beam-column joints: State of the art", *ACI Struct. J.*, **102**(2).
- Fanaie, N., Esfahani, F.G. and Soroushnia, S. (2015), "Analytical study of composite beams with different arrangements of channel shear connectors", *Steel Compos. Struct., Int. J.*, **19**(2), 485-501.
- Hadi, M.N. and Tran, T.M. (2016), "Seismic rehabilitation of reinforced concrete beam-column joints by bonding with concrete covers and wrapping with FRP composites", *Mater. Struct.*, **49**(1-2), 467-485.
- Hosseinpour, E., Baharom, S., Badaruzzaman, W.H.W., Shariati, M. and Jalali, A. (2018), "Direct shear behavior of concrete filled hollow steel tube shear connector for slim-floor steel beams", *Steel Compos. Struct., Int. J.*, **26**(4), 485-499.
- Hui, Y. and Irawan, P. (2001), "Behaviour of full-scale lightly reinforced concrete beam-column joints", *Civil Engineering Research*; Nanyang Technological University, Singapore, pp. 44-45.
- Ismail, M., Shariati, M., Awal, A., Chiong, C., Chahnasir, E., Porbar, A., Heydari, A. and Khorami, M. (2018), "Strengthening of bolted shear joints in industrialized ferrocement construction", *Steel Compos. Struct., Int. J.*, **28**(6), 681-690.
- Khorramian, K., Maleki, S., Shariati, M. and Ramli Sulong, N.R. (2015), "Behavior of Tilted Angle Shear Connectors", *PLoS one*, **10**(12), 1-11.
- Khorramian, K., Maleki, S., Shariati, M., Jalali, A. and Tahir, M.M. (2017), "Numerical analysis of tilted angle shear connectors in steel-concrete composite systems", *Steel Compos. Struct., Int. J.*, **23**(1), 67-85.
- Lee, H.-J. and Hwang, J.-S. (1999), "A study on the effect of fracture delay of intelligent FRP by transparent photoelastic experimental method", *Transact. Kor. Soc. Mech. Eng. A*, **23**(11), 1904-1911.
- McCormac, J.C. and Brown, R.H. (2015), *Design of Reinforced Concrete*, John Wiley & Sons.
- Mohammadhassani, M., Suhatri, M., Shariati, M. and Ghanbari, F. (2014), "Ductility and strength assessment of HSC beams with varying of tensile reinforcement ratios", *Struct. Eng. Mech., Int. J.*, **48**(6), 833-848.
- Nasrollahi, S., Maleki, S., Shariati, M., Marto, A. and Khorami, M. (2018), "Investigation of pipe shear connectors using push out test", *Steel Compos. Struct., Int. J.*, **27**(5), 537-543.
- Nordin, H. (2005), "Strengthening structures with externally prestressed tendons: literature review."
- Sadeghipour, E.S., Zandi, Y., Shariati, M., Dehghani, E., Togholi, A., Mohamed, E.T., Shariati, A., Safa, M., Wakil, K. and Khorami, M. (2018), "Application of support vector machine with firefly algorithm for investigation of the factors affecting the shear strength of angle shear connectors", *Smart Struct. Syst., Int. J.*, **22**(4), 413-424.
- Safa, M., Shariati, M., Ibrahim, Z., Togholi, A., Baharom, S.B., Nor, N.M. and Petkovic, D. (2016), "Potential of adaptive neuro fuzzy inference system for evaluating the factors affecting steel-concrete composite beam's shear strength", *Steel Compos. Struct., Int. J.*, **21**(3), 679-688.
- Sedghi, Y., Zandi, Y., Togholi, A., Safa, M., Mohamad, E.T., Khorami, M. and Wakil, K. (2018), "Application of ANFIS technique on performance of C and L shaped angle shear connectors", *Smart Struct. Syst., Int. J.*, **22**(3), 335-340.
- Shahabi, S.E.M., Ramli Sulong, N.H., Shariati, M.,

- Mohammadhassani, M. and Shah, S.N.R. (2016a), "Numerical analysis of channel connectors under fire and a comparison of performance with different types of shear connectors subjected to fire", *Steel Compos. Struct., Int. J.*, **20**(3), 651-669.
- Shahabi, S., Sulong, N., Shariati, M. and Shah, S. (2016b), "Performance of shear connectors at elevated temperatures-A review", *Steel Compos. Struct., Int. J.*, **20**(1), 185-203.
- Shariati, M. (2013), "Behaviour of C-shaped Shear Connectors in Steel Concrete Composite Beams", Jabatan Kejuruteraan Awam, Fakulti Kejuruteraan, Universiti Malaya.
- Shariati, M., Ramli Sulong, N.H., Sinaei, H., Arabnejad, K.M.M., Mehdi, M. and Shafiqh, P. (2011), "Behavior of Channel Shear Connectors in Normal and Light Weight Aggregate Concrete (Experimental and Analytical Study)", *Adv. Mater. Res.*, **168**, 2303-2307.
- Shariati, A., Ramli Sulong, N.R., Suhatrik, M. and Shariati, M. (2012a), "Investigation of channel shear connectors for composite concrete and steel T-beam", *Int. J. Phys. Sci.*, **7**(11), 1828-1831.
- Shariati, M., Ramli Sulong, N., Suhatrik, M., Shariati, A., Arabnejad Khanouki, M. and Sinaei, H. (2012b), "Fatigue energy dissipation and failure analysis of channel shear connector embedded in the lightweight aggregate concrete in composite bridge girders", *Proceedings of the 5th International Conference on Engineering Failure Analysis*, The Hague, The Netherlands, July.
- Shariati, M., Ramli Sulong, N.R., Suhatrik, M., Shariati, A., Khanouki, M.A. and Sinaei, H. (2012c), "Behaviour of C-shaped angle shear connectors under monotonic and fully reversed cyclic loading: An experimental study", *Mater. Des.*, **41**, 67-73.
- Shariati, M., Shariati, A., Ramli Sulong, N.R., Suhatrik, M. and Arabnejad, K.M.M. (2014), "Fatigue energy dissipation and failure analysis of angle shear connectors embedded in high strength concrete", *Eng. Fail. Anal.*, **41**, 124-134.
- Shariati, M., Ramli Sulong, N.R., Shariati, A. and Arabnejad, K.M.M. (2015), "Behavior of V-shaped angle shear connectors: experimental and parametric study", *Mater. Struct.*, **49**(9), 3909-3926.
- Shariati, M., Ramli Sulong, N.R., Shariati, A. and Kueh, A.B.H. (2016), "Comparative performance of channel and angle shear connectors in high strength concrete composites: An experimental study", *Constr. Build. Mater.*, **120**, 382-392.
- Shariati, M., Toghrol, A., Jalali A. and Ibrahim, Z. (2017), "Assessment of stiffened angle shear connector under monotonic and fully reversed cyclic loading", *Proceedings of the 5th International Conference on Advances in Civil, Structural and Mechanical Engineering - CSM 2017*, Zurich, Switzerland.
- Tahmasbi, F., Maleki, S., Shariati, M., Ramli Sulong, N.R. and Tahir, M.M. (2016), "Shear capacity of C-shaped and L-shaped angle shear connectors", *PloS one*, **11**(8), e0156989.
- Tang, W.C., Balendran, R.V., Nadeem, A. and Leung, H.Y., (2006), "Flexural strengthening of reinforced lightweight polystyrene aggregate concrete beams with near-surface mounted GFRP bars", *Build. Environ.*, **41**(10), 1381-1393.
- Thomas, P. and Priestley, M. (1992), *Seismic Design of Reinforced Concrete and Masonry Buildings*, New York Wiley-Interscience, USA.
- Wang, M., Shi, X., Zhou, J. and Qiu, X. (2018), "Multi-planar detection optimization algorithm for the interval charging structure of large-diameter longhole blasting design based on rock fragmentation aspects", *Eng. Optimiz.*, **50**(12), 2177-2191.
- Wang, M., Shi, X. and Zhou, J. (2019), "Optimal Charge Scheme Calculation for Multiring Blasting Using Modified Harries Mathematical Model", *J. Perform. Constr. Facil.*, **33**(2), 04019002.
- Wei, X., Shariati, M., Zandi, Y., Pei, S., Jin, Z., Gharachurlu, S., Abdullahi, M.M., Tahir, M.M. and Khorami, M. (2018), "Distribution of shear force in perforated shear connectors", *Steel Compos. Struct., Int. J.*, **27**(3), 389-399.
- Zhou, J., Li, E., Wang, M., Chen, X., Shi, X. and Jiang, L. (2019), "Feasibility of Stochastic Gradient Boosting Approach for Evaluating Seismic Liquefaction Potential Based on SPT and CPT Case Histories", *J. Perform. Constr. Facil.*, **33**(3), 04019024.

CC